KIEL-UP • DOI: 10.38072/2748-3150/p37

What do we learn from ground level enhancements?

Athanasios Papaioannou

Correspondence
IAASARS – Institute for Astronomy, Astrophysics, Space Applications and Remote Sensing, National Observatory of Athens, Penteli, Greece, atpapaio@astro.noa.gr

Keywords
solar energetic particles; ground level enhancements; coronal mass ejections; solar flares; neutron monitors

Abstract
Ground level enhancements (GLEs) comprise the high-energy end of solar energetic particle (SEP) events and constitute a special class in which ions are accelerated to relativistic energies, causing a significant sudden increase of cosmic rays at ground-based detectors, mainly at neutron monitors (NMs). GLEs require acceleration processes capable of producing particles with sufficient energy to allow their secondary products to reach the terrestrial ground and be detected. Moreover, due to their fast propagation, relativistic protons in GLEs are particularly useful for the identification of SEP sources at the Sun (i.e. flare, coronal mass ejections) – nonetheless, the debate about the exact nature of GLE mechanisms is still ongoing. GLEs are further critical for the establishment of Space Weather services and the accurate determination of their imposed radiation risk. In this tutorial, an overview of GLEs with respect to their historical identification, measurements from the worldwide neutron monitor network, modeling and forecasting efforts will be provided. In addition, a hands-on tutorial that will demonstrate how the Neutron Monitor Database (NMDB) can be utilized for GLE analysis will be conducted.

1. Introduction

Ground level enhancements (GLEs) are short-term increases of the cosmic ray intensity above the ever-present background of galactic cosmic rays registered at the ground by particle detectors (usually neutron monitors – NMs; Miroshnichenko, 2001; Poluianov et al. 2017) (see Figure 1). These particles originate at the Sun and are very fast (i.e. reach near-relativistic energies). GLEs are associated with solar eruptive events such as solar flares and coronal mass ejections (CMEs). A central scientific question which is still under debate up to nowadays concerns the mechanisms responsible for the production of these near-relativistic protons that give rise to GLEs.

KIEL-UP • DOI: 10.38072/2748-3150/p37

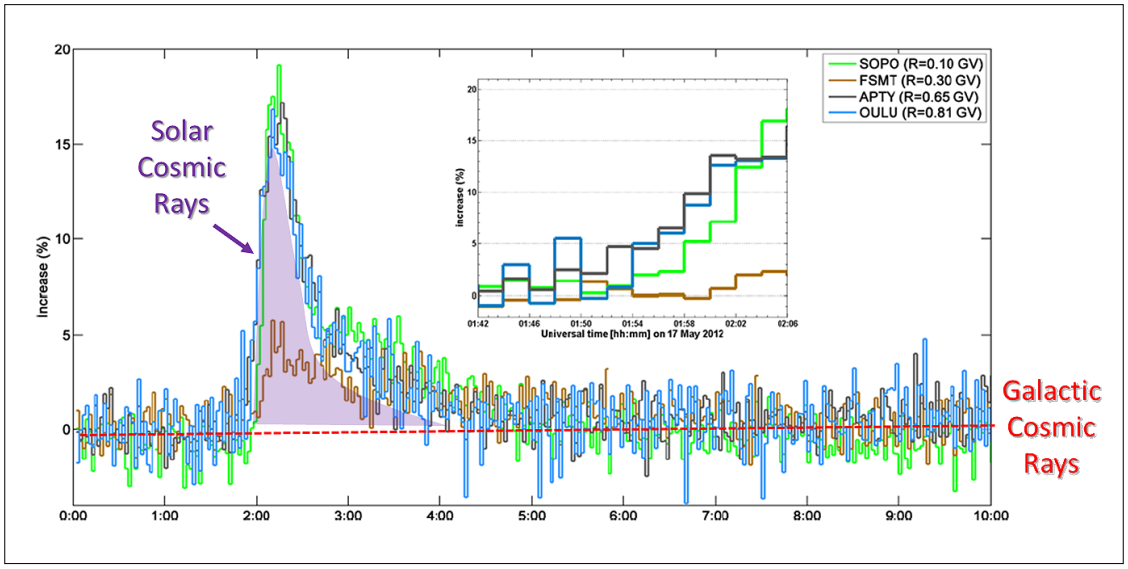

Fig. 1: Recordings of GLE71 on 17 May 2012 by South Pole (SOPO), Fort Smith (FSMT), Apatity (APTY) and Oulu (OULU) NMs. The red dashed horizontal line depicts the average galactic cosmic ray background and the shaded purple area the excess of solar cosmic ray particles that constitute this GLE event (adapted from Papaioannou et al. 2014).

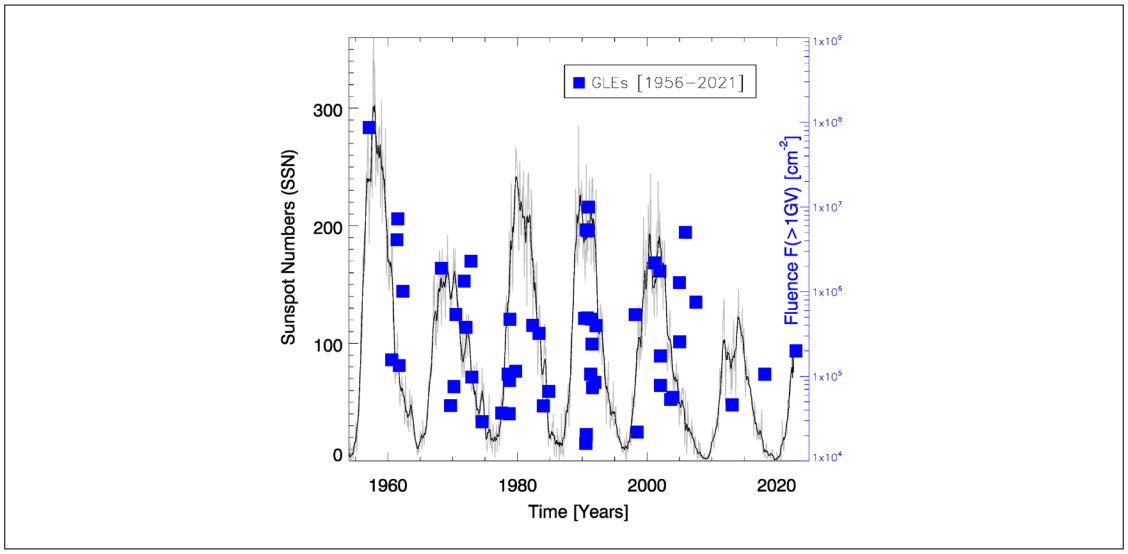

Fig. 2: Distribution over time of 68 GLEs since 1956, on the background of the evolving solar cycle. The blue squares depict the fluence F(>1 GV) for each GLE.

GLEs constitute the most energetic class of solar energetic particle (SEP) events. They were first discovered by Forbush (1946) who identified three unusual cosmic ray increases and further linked them to charged particles emitted from the Sun. A few years later with the implementation of NMs Meyer, Parker and Simpson (1956) studied the GLE that was recorded on 23 February 1956 (GLE05) indicating solar flares as the driving source of these particles. GLE05 is the largest GLE event to date (see Usoskin et al. 2020, Mallios et al. 2022). GLEs are rare events since from 1946 there have only been 73 such events (or 68 if the counting starts at the NM era, i.e. GLE05 onwards) leading to a rate of ~1.04 GLEs/yr. Figure 2 depicts all

KIEL-UP • DOI: 10.38072/2748-3150/p37

68 GLEs since 1956 through their achieved fluence at >1GV (F(>1GV) in cm^{-2}; y-axis on the right) plotted on the background of the evolving solar cycle which in turn is presented through the sunspot number (SSN; y-axis on the left). One may notice that GLE05 achieved a fluence almost one order of magnitude larger than all other GLEs up until today. Moreover, although GLEs follow the solar cycle (SC) evolution, in general, they seem to be present not only in the maximum but also in the ascending and declining phases of the SC. Finally, SC24 (after 2006) was the weakest SC presented and the origin of only two GLE events.

2. From the Sun to the ground

Multiple steps and building blocks need to be taken into account in order to understand and evaluate the physics of high-energy particle acceleration, injection and transport in the inner heliosphere, the interaction of these particles with the magnetosphere and the atmosphere of the planet (in our case, the Earth), as well as, the pivotal role of GLEs and ground based detectors, i.e. NMs. This is because GLE near-relativistic particles (i.e. "primary" solar cosmic ray particles) are accelerated at the Sun, propagate in interplanetary space and – once they reach the magnetopause – enter the magnetosphere where their particle trajectories bent. Consequently they enter the atmosphere and interact with its molecules creating a cascade that leads to the "secondary" solar cosmic rays. In turn, these secondary products eventually are recorded by a NM. Hence, it becomes apparent that taking all of the aforementioned steps into consideration is vital in the understanding of the underlying physics at every step. What is more, GLE recordings are most appropriate to shed light on the problem of particle acceleration, since those: (a) frame the early phase of SEP events – close to the time of acceleration and (b) the role of interplanetary transport is assumed to be minimal on the scattering of the particles (i.e. focused transport of near-relativistic particles).

2.1 The Sun is the giver of (life) particles

Paraphrasing Ramses the II, the Sun is the giver of particles. For hundreds of years people are looking at the Sun, drawing and monitoring its sunspots (Cliver and Herbst 2018). Modern instrumentation allowed scientists to get unprecedented imaging of the Sun and its dynamics, providing insights to concepts of i.e. the solar cycle variation and the eruption of solar flares and CMEs. Figure 3 shows a combination of both these solar eruptive events. In particular, (from left to right), actual observations of a solar flare recorded by the Solar Dynamic Observatory (SDO) on 2012-05-17, a 2D model of stochastic acceleration in solar flares; magnetic field lines (in green) and turbulent plasma or plasma waves (as red circles) generated during magnetic reconnection (highlighted with a red circle). Blue arrows heading back to the solar surface depict accelerated particles impinging on the lower denser chromosphere, while similar arrows heading upwards present accelerated particles that may escape to interplanetary space. These are then detected as SEPs and/or GLEs (adapted from Vlahos et al. 2019; Temmer 2021) and a CME on the same date observed by the Solar and Heliospheric Observatory (SOHO); an emerging CME-driven shock (black arc) that may also accelerate SEPs/GLEs (black dots) in the corona or heliosphere via diffusive shock acceleration (highlighted with a red circle; adapted from Mikić and Lee 2006; Temmer 2021).

During a solar flare, electromagnetic radiation covering the whole electromagnetic spectrum is generated by the hot plasma and the non-thermal particles and travels at the speed of light through the interplanetary space. Usual indicators of solar flares lie in the X-ray and the radio emissions. This type of

KIEL-UP • DOI: 10.38072/2748-3150/p37

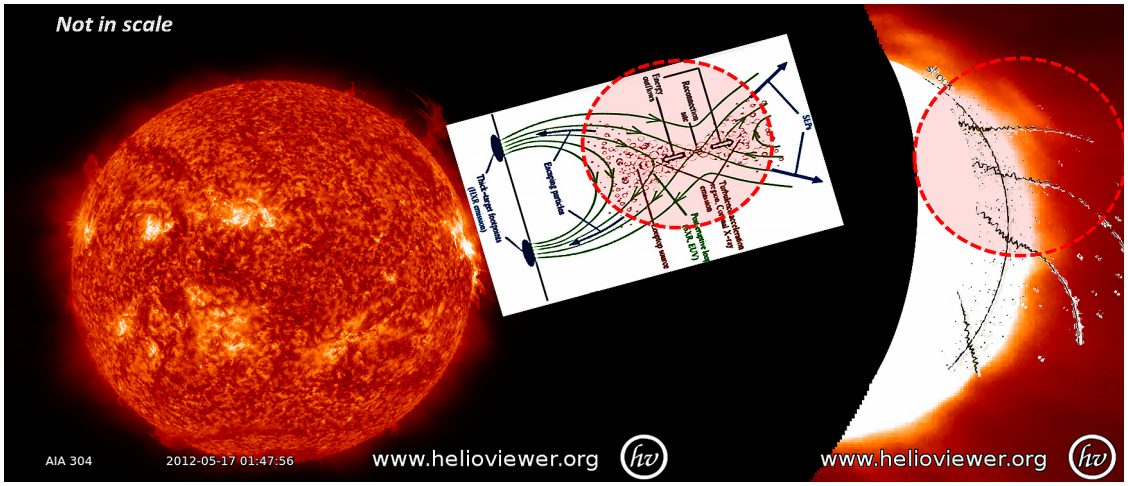

Fig. 3: A composite figure demonstrating the two major solar eruptive events (i.e. solar flare and CME) for GLE71 (17/05/2012) (made with https://www.jhelioviewer.org), as well as the dominant acceleration mechanisms, i.e. stochastic acceleration in solar flares (adapted from Vlahos et al. 2019) and DSA in propagating bow shocks (adapted from Mikić and Lee 2006). The red dashed circles demonstrate the acceleration sites.

radiation travels radially from the Sun to the Earth and requires ~8.33 minutes to reach the observing point (at Earth). The onset of an increase in soft X-ray (SXR) emission detected by sensors on the Earth-orbiting spacecraft is approximately simultaneous with the visual observations of a solar flare (see Figure 3, left panel) usually made in the Hα wavelength. CMEs are sudden expulsions of magnetized plasma into the solar wind from regions initially magnetically closed. These form in the low corona (below ~ 2 Rs) and their energies range up to ~ 10^{31} - 10^{32} erg, and their mass up to ~ 10^{35} erg. The average speed of CMEs is ~500 km/s and their width is ~ 50 degrees (Vourlidas 2021). Most CMEs are in general associated with some level of X-ray emission, although, there are many more flares than CMEs. Nonetheless the strongest flares (in terms of magnitude) are most probably associated with CMEs, since solar eruptive events do not evolve in isolation but in concert, as a result of changes in the magnetic field (Yashiro et al. 2006). Radio waves from the Sun indicate electron acceleration, primarily to energies of tens of keV, and such electrons are likely to be accelerated at any time that high energy ions are accelerated. The characteristics of solar radio emissions as a function of frequency and time, at frequencies below a few hundred MHz, have been described in terms of five main types of bursts named type I through V (Wild et al. 1963). The most common types are: (a) type III burst, a classic signature of the so-called "impulsive phase" of flares which signify the opening of the magnetic field lines allowing the release of particles to the interplanetary medium[1] and (b) type II bursts denoted by their slow drift, implying speeds appropriate for coronal shock waves, and thus related to CMEs (Klein 2021a,b).

2.2 The Sun-Earth connection for energetic particles

Unlike solar electromagnetic radiation, those particles that are accelerated and injected into interplanetary space need to be directed to the appropriate interplanetary magnetic field (IMF) line that connects the source at the Sun to the observer at Earth. That said, both the onset time and the obtained maximum

1 Type III bursts trace electron streams as they propagate along open field lines from flaring regions near the Sun into the interplanetary medium. Nonetheless, a study by e.g. Benz et al. (2005) suggests that only in a third (33%) of all flares (>C5.0) at least one of the four ends of reconnecting field lines is open.

KIEL-UP • DOI: 10.38072/2748-3150/p37

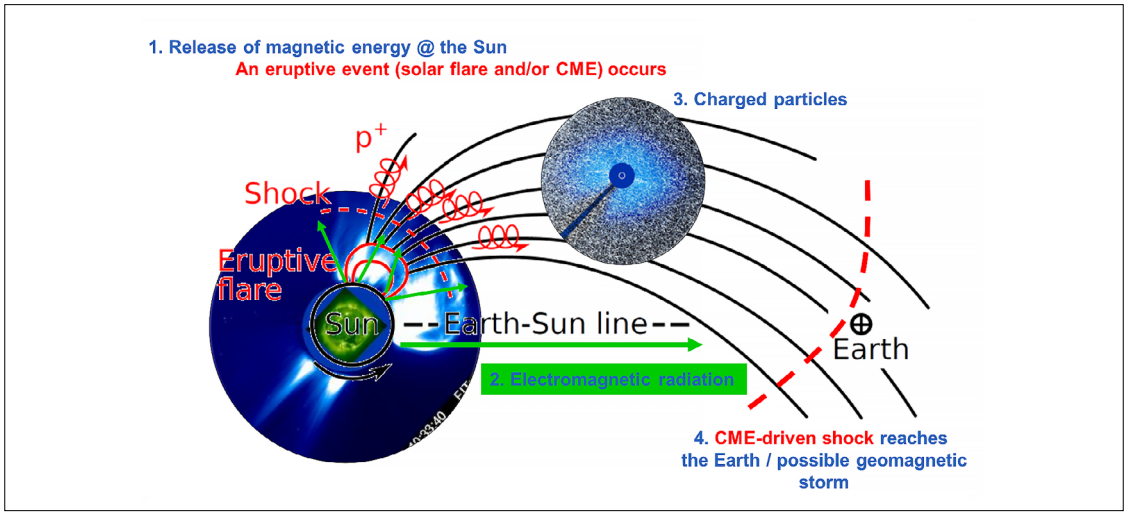

Fig. 4: A schematic of the solar storm scenario divided into 4 steps. A solar eruptive event initiates the scenario [1], its electromagnetic signatures arrive at the detector/observer [2], charged particles [3] are released and spiral along the IMF lines and if the CME drives a shock, when that reaches the Earth a geomagnetic storm may occur [4].

intensity of an SEP/GLE at a given (detection) point in the interplanetary space is dependent on the particles' source. This means that the location (i.e. helio-longitude) of the parent solar flare of an SEP/GLE with respect to the detection point is very important. This is explained as follows: first of all, as it is known, the IMF topology is governed by the solar wind outflow and the rotation of the Sun. As a result, during so-called "quiet" conditions (when the solar wind speed ranges from 300-400 km/s) the IMF can be approximated by an Archimedean (or a Parker) spiral, the nominal length of which is ~1.2 AU. Second of all, the previously accelerated and injected particles into the interplanetary medium, being charged, spiral along the IMF lines. Thereby, a favorable magnetic connection is established between the Earth and solar flares that occur at the Sun's W50-W70 helio-longitude, being termed as "well-connected" ones. In this picture one may further add a propagating CME that drives a shock. SEPs time-intensity profiles are organized in terms of the longitude of the observer with respect to the solar source (Cane and Lario 2006), in general, and the CME-driven shock (Cane et al. 1988), in particular, and thus particles are able to propagate to remote observers within the inner heliosphere.

Another important aspect is the energy of the released particles. For example, for the propagation along a nominal Archimedean spiral (i.e. scatter-free propagation) from the Sun to the Earth, 10 MeV protons take ~70 minutes; 100 MeV ~24 minutes and 450 MeV ~14 minutes to cover the same distance. That said, the higher the energy of the particles the less time they require to reach the Earth and in turn, near-relativistic protons recorded by NMs offer a prime sample for the investigation of the acceleration mechanisms at play. Figure 4 presents a combined scenario distributed over 4 steps taking into account the aforementioned facts.

2.3 Flare versus CME-shocks for GLEs

The open scientific question that rose decades ago and is still under debate focuses on the dominant acceleration mechanism for GLEs. For example, studies indicated that relativistic particles can be accelerated either through a coronal shock driven by the CME (see e.g. Vainio & Laitinen 2007, Afanasiev et

KIEL-UP • DOI: 10.38072/2748-3150/p37

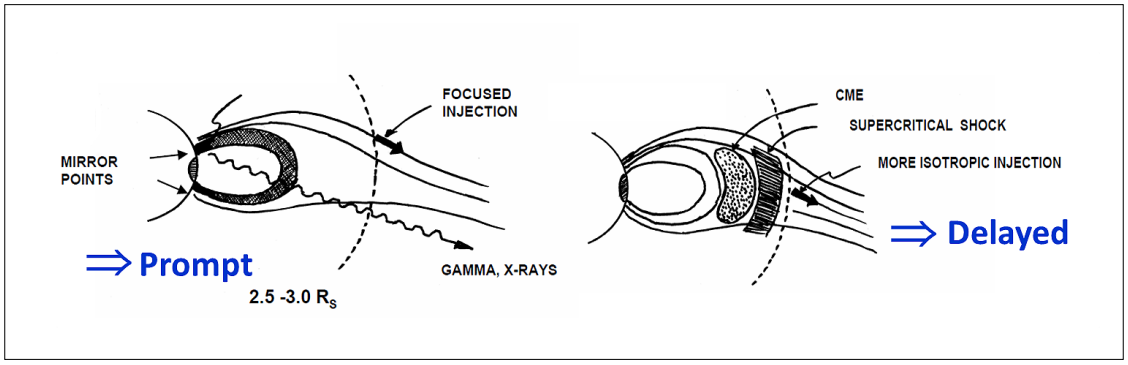

Fig. 5: A schematic of the prompt and focussed injection of particles following a solar flare giving ground to the "prompt" component of GLEs, followed by the expansion of a CME that leads to supercritical shock and results in a more isotropic injection giving ground to the "delayed" component of a GLE (adapted from Moraal and McCracken 2012).

al. 2018), or through magnetic reconnection during a flare (see a recent review in e.g. Vlahos et al. 2019). The observational findings that point to a flare origin are summarized as: (a) powerful flares are always present during GLEs; (b) the flare versus GLE timing has an excellent correlation; (c) no (significant) correlation of the fluence of GLEs with the CME speed and (d) favorable longitudinal distribution of the parent flares (the majority for GLEs are "well-connected" ones). On the opposite site, observational findings pointing to a CME origin are: (a) the majority of GLEs is associated with most powerful CMEs; (b) close connection with a type II radio emission which is indicative of a shock; (c) a delay between the flare's timing and the particle's escape into interplanetary space – depending on energy and (d) long injection comparatively to the impulsive phase of a flare. Nonetheless, since GLEs always occur after a very strong solar flare and a fast and wide CME (see e.g. Gopalswamy et al. 2012) a clear-cut separation has not been achieved up until today. Thereby each GLE event is treated separately (see some recent studies in e.g. Klein et al. 2022; Mishev et al. 2022; Papaioannou et al. 2022). Moreover, the pioneer work of Vashenuyk et al. (2011) introduced the so-called "prompt" and the "delayed" components scenario for GLEs, with the former being driven by the flare and the latter by the CME (see also McCracken et al. 2012; Figure 5).

2.4 Propagation in the magnetosphere

The motion of a charged particle in the magnetosphere is governed by the Lorentz force, that is, that the trajectories of particles are bent by the Earth's magnetic field. Numerical methods employing a model of the magnetic field are required for the calculation of the particles' trajectories in the magnetosphere (Smart et al. 2000). The magnetic field of the Earth is represented with two parts: the inner one generated by an internal dynamo and the outer part induced by different current systems in the ionosphere and the magnetosphere accounting for the interaction of the Earth's magnetic field with the solar wind (e.g. Bütikofer 2018 and references therein). For the internal magnetic field, the International Geomagnetic Reference Field (IGRF) model is usually employed while for the external magnetic field the semi-empirical model by Tsyganenko et al. (1989) (TSY89) requiring as the only input the geomagnetic activity index Kp is usually used (see e.g. discussion in Herbst 2021 and references there in). The geomagnetic field provides a shield against charged particles, which is most effective near the geomagnetic equator and marginal or almost non-present near the geomagnetic poles. Therefore, the access of energetic particles at a specific point of observation within the magnetosphere is determined by: (a) the Earth's magnetic field, (b) the energy

KIEL-UP • DOI: 10.38072/2748-3150/p37

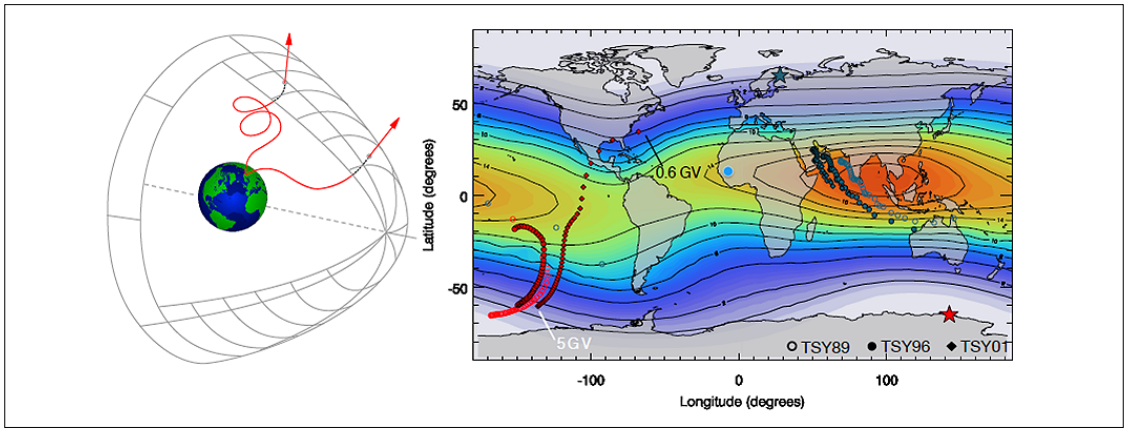

Fig. 6: An illustration of the concept of the asymptotic cones (taken from Herbst 2021).

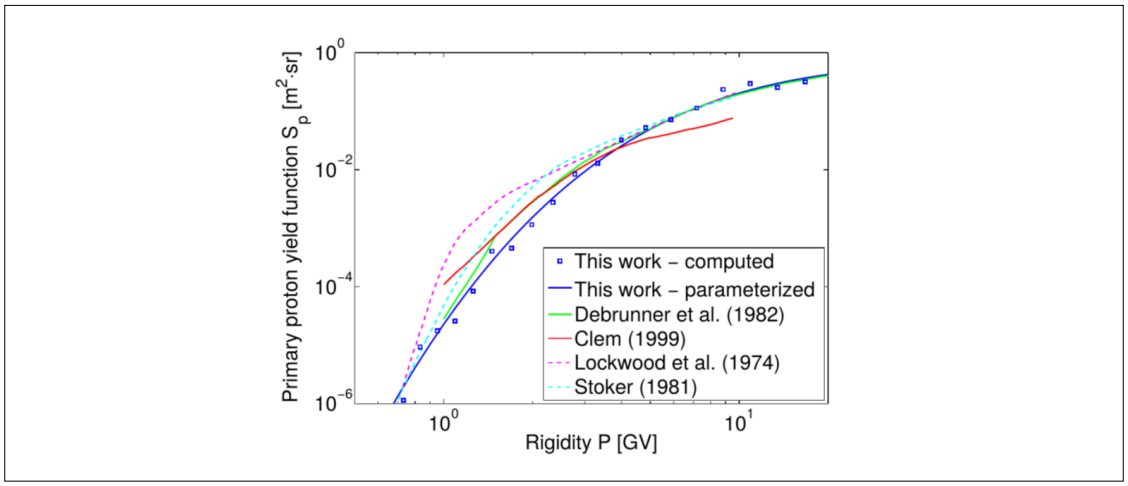

Fig. 7: Comparison of the NM yield function (taken by Flückiger et al. 2008).

and (c) the incidence angle of the particle. Usually, this access is quantified by the effective cut-off rigidity, R_c (R_c=p_c/Z_e, where p is the momentum, c is the speed of light and Z_e is the charge of the particle; units GV), which is defined as the rigidity below which particles have no access to this location. Therefore, the trajectories of particles with rigidities greater (below) than R_c are "allowed" ("forbidden"). Moreover, the asymptotic direction of the incoming particles is used as the particle's trajectory direction of approach at the boundary of the magnetosphere. The geomagnetic cut-off varies from 0 to 17 GV (~17 GeV in energy for protons).

2.5 Propagation in the atmosphere

The transport of particles in the Earth's atmosphere depends on the atmospheric depth or atmospheric cut-off which is the lower energy limit of particles that can reach a given location on the ground and be registered by a NM. This cut-off is about 1 GV (~433 MeV in energy for protons). Nonetheless, the atmospheric cut-off decreases with altitude, and thus provides additional sensitivity of high-altitude polar neutron monitors to low-energy particles, mainly during GLEs pushing the lower-energy limit to ~ 300 MeV (see Poluianov and Batalla 2022). As noted here above, once a "primary" particle enters the atmosphere it

KIEL-UP • DOI: 10.38072/2748-3150/p37

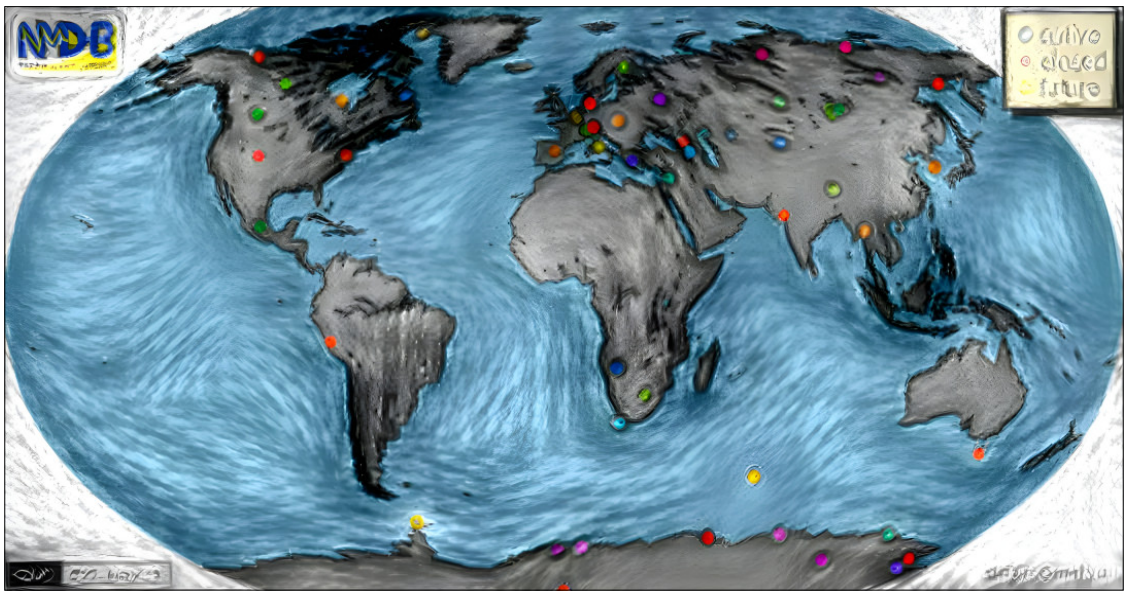

Fig. 8: Image of the distribution of the neutron monitors on the world map (credit: NMDB; http://nmdb.eu) treated with an artificial intelligence filter called Deep Dream technology (https://deepdreamgenerator.com/).

interacts with its molecules producing an atmospheric cascade and results to "secondary" particles. The intensity of the cascade (i.e. the number of secondary particles) grows with the growing atmospheric depth, until a maximum is reached. Thereafter it exponentially decreases. That said, it becomes apparent that a more energetic "primary" particle induces a stronger atmospheric cascade with a higher probability to reach the ground, and be measured by a NM. The unfolding of the cascade in the atmosphere and the NM detection efficiency for secondary cosmic ray particles are combined in the NM yield function (see Figure 7) (Flückiger et al. 2008; Mishev et al. 2013, 2020).

3. Analysis of GLEs by neutron monitor measurements

3.1 The neutron monitor network

Neutron monitors record secondary particles and the NM location corresponds to primaries: (a) with energies covering a specific part of the primary spectrum depending on the cut-off rigidity of the location and (b) coming from a specific set of directions. Thereby the usage of all available neutron monitors offers a more complete picture of the angular and energy distribution of the primary particles. That said the Network of NMs (Figure 8) serves as a Multi-directional tool, revealing the properties of primary particles reaching the Earth's atmosphere. Almost 15 years ago, the implementation of the Neutron Monitor Database (NMDB; https://www.nmdb.eu) provided the opportunity to gather high-quality fine resolution (1-min) NM data in real-time mode, directly addressing the need for timely Space Weather related applications and archived data with higher time resolution that facilitates long-term investigations of the solar-terrestrial relations (Mavromichalaki et al. 2011; Steigies and Fuller 2023).

KIEL-UP • DOI: 10.38072/2748-3150/p37

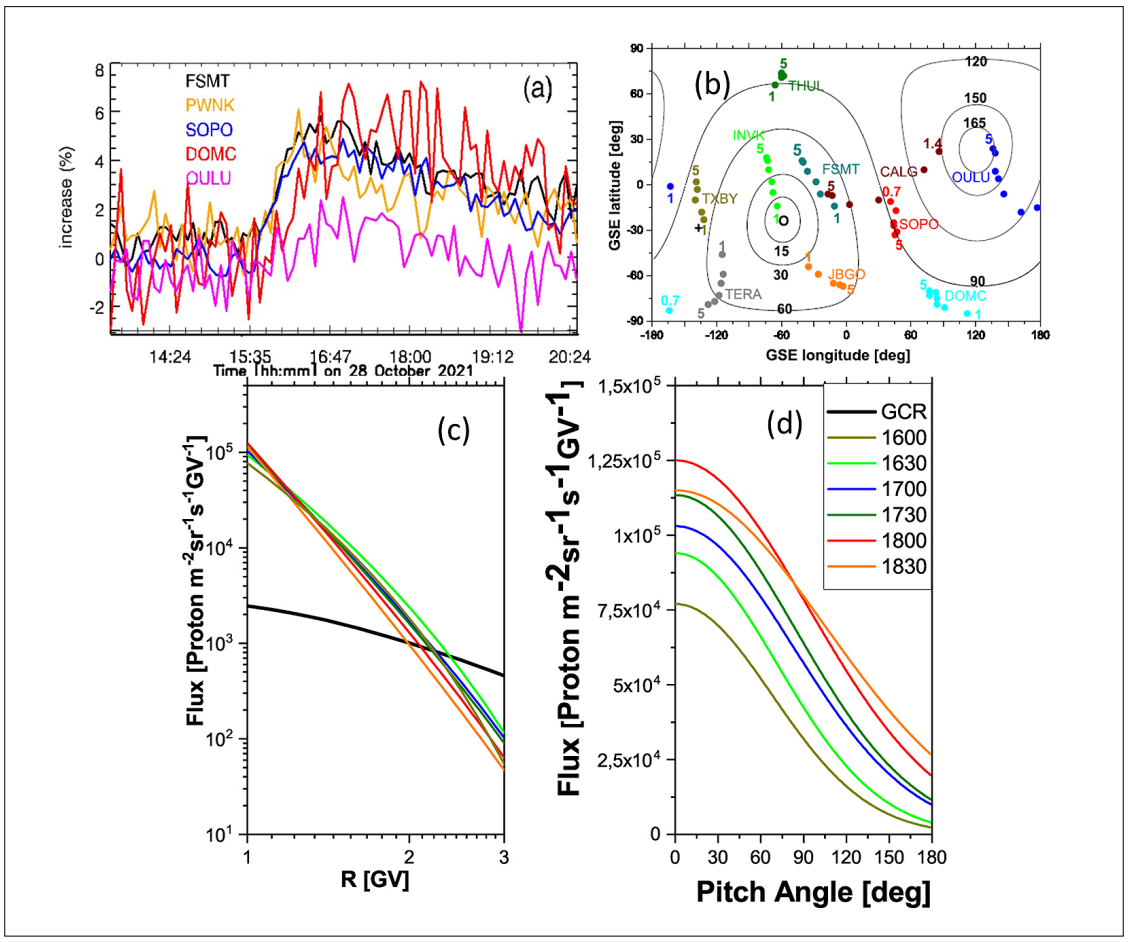

Fig. 9: Composite picture of the GLE analysis/modeling: (a) GLE73 recordings of NMs; (b) calculated asymptotic directions for GLE73 (from Mishev et al. 2022); (c) modeled spectrum of GLE73 and (d) modeled pitch-angle distribution for GLE73 (from Papaioannou et al. 2022).

3.2 Modeling GLEs

The analysis of GLEs requires the modeling of the response (i.e. recordings) of an adequate (optimally a significant number of NMs with good spatial coverage around the world and with quality data) number of NMs aiming at determining an optimal fit for the SEP spectrum and the angular distribution at 1 AU (see Mishev et al. 2022 and references therein). The usage of the worldwide network of neutron monitors is ideal for this task, since NMs situated in different geographic regions are sensitive to a different part of the solar particle spectra and arrival direction (Mishev and Usoskin 2020). This is basically achieved via a three-step procedure:

- *First step*: Compute the asymptotic directions and the cut-off rigidity of NM stations, i.e. simulate the propagation of the charged particles in a modeled magnetosphere.
- *Second step*: Make an initial guess of the inverse problem by viable assumptions keeping in mind that functions need to represent the physical processes involved.
- *Third step*: Apply an optimization method and identify the energy spectrum, the anisotropy axis direction and the pitch-angle distribution.

KIEL-UP • DOI: 10.38072/2748-3150/p37

The model of the global response of NMs during a GLE has been developed over many years (e.g. Shea and Smart 1982; Flückiger & Kobel 1990; Belov et al. 2005; Bieber et al. 2013; Bombardieri et al. 2008; Bütikofer et al. 2008, 2016; Plainaki et al. 2007, 2010; Vashenyuk et al. 2011; Mishev et al. 2018, 2022) and is described in detail by Cramp et al. (1997). This method employs a least-squares fitting technique to determine the axis of symmetry of the particle arrival, the spectrum and the anisotropy of the high-energy solar protons that give rise to the increased neutron monitor response.

The spectral shape of the "primary" particles needs to be assumed in such a process. This is directly related to the acceleration process involved. Several such forms have been investigated, as pure and modified power laws, as well as spectra based on theoretical expectations (Ellison and Ramaty 1985). An empirical functional form that can be employed to fit the neutron monitor observations is the so-called: "modified power-law" spectrum which incorporates the change of the power law exponent ($\delta\gamma$), leading to a spectrum that steepens with increasing rigidity (see Mishev et al. 2022; Papaioannou et al. 2022 and references therein).

The propagation of particles through the interplanetary medium results in a distribution of pitch angles which can be described using a functional form. Formally, the particle pitch angle is defined as the angle between the axis of symmetry of the particle distribution and the asymptotic direction of view. The most widely-used functions have been cosine or Gaussian relationships (see Cramp et al. 1997; Mishev et al. 2022). Figure 9 depicts results from the analysis and modeling of the recent GLE73.

3.3 Forecasting solar storms

Since the propagation of particles is governed by their energy (speed) the near-relativistic particles that are recorded by NMs are the fastest and establish a distinguishable enhancement at the ground level prior to the arrival of the bulk of the several 10's of MeV particles that follow. Therefore one can make use of the particle recordings at NMs in order to forecast the arrival of lower energy protons (see details in e.g. Kuwabara et al. 2006; Souvatzoglou et al. 2014), as this is illustrated in Figure 10 (left panel) which shows the NM recordings of GLE60 on 15 April 2001 compared to the GOES spacecraft measurements at E>10 and E>100 MeV (Kuwabara et al. 2006). As it can be seen, the first arriving particles at the ground provide an earlier onset compared to the time when the enhancement was clearly identified in spacecraft measurements. Thereby, the time difference provides a window of reliable forecasting based solely on NM measurements giving ground to the so-called "GLE Alert". Figure 10 (right panel) shows the velocity dispersion analysis (VDA; Vainio et al. 2013; Paassilta et al. 2017) for GLE31 on 07 May 1978. VDA assumes that particles at all energies exhibit a simultaneous release into the interplanetary medium follow the IMF lines and arrive promptly to the observer (i.e. Earth). Due to this scenario (see also Section 2) the onset times of these solar particles at different energies as a function of their inverse velocity leads to a linear fit, with the slope of the fit providing the path length travelled by the particles and the intersection with the y-axis denoting the solar release time.

Once a "GLE Alert" is established then NMs can further provide an estimation of the expected spectrum down to lower-energies and most importantly can inform about the radiation hazard at flight altitudes due to the forthcoming increased exposure, particularly during long flights at low cut-off rigidities, e.g. over the polar and sub-polar regions (Mishev and Velinov 2020).

KIEL-UP • DOI: 10.38072/2748-3150/p37

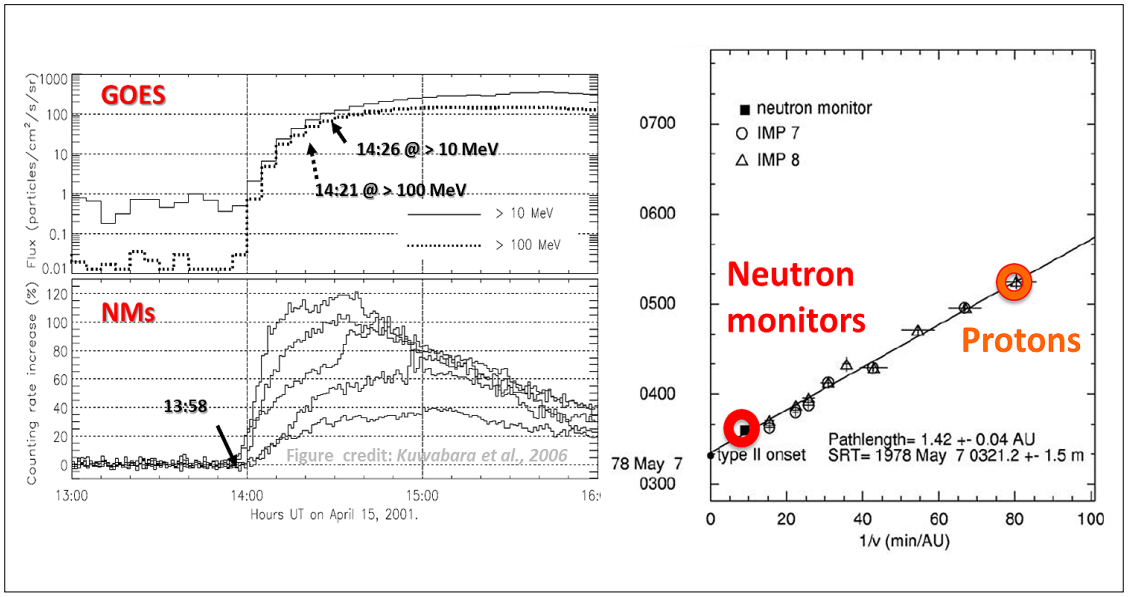

Fig. 10: Left panel: Recordings of the GLE60 on 15 April 2001 by NMs (bottom) and by GOES spacecraft (upper plot; adapted from Kuwabara et al. 2006). Velocity Dispersion Analysis (VDA) of GLE31 on 07 May 1978 based on spacecraft (IMP7 & IMP8) and neutron monitor measurements (adapted from Reames 2009).

4. Analysis of GLEs in the inner heliosphere

Particles emitted from the Sun, reaching to GLE energies (E>430 MeV or E>300 MeV for high altitude polar NMs) are recorded as excesses of solar particles above the background since the start of the space era. These data have been obtained from particle sensors on near-Earth satellites and on space probes throughout the heliosphere. When these observations are coupled with NM recordings they greatly increase our understanding of the fundamental processes of the generation of solar energetic particles and their propagation in the interplanetary medium.

4.1 Recordings at spacecraft detectors

From the patrol measurements offered by the Geostationary Operational Environmental Satellite (GOES) series, the High Energy Proton and Alpha Detector (HEPAD) could register particles up to 700 MeV. Thereby, GOES observations have been used for the identification of a number of GLEs at a range from ~10-700 MeV (Figure 11, left panel; e.g. Mishev et al. 2018; Rodriguez and Kress 2023). Moreover, such recordings led to the unfolding of the spectrum during GLEs and demonstrated a double power-law behavior with a characteristic "break" energy (Figure 11, right panel, see details in Mewaldt et al. 2012; Cohen and Mewaldt 2018) which has been explained either on the basis of the CME-shock acceleration, transport of solar particles and/or on the existence of two distinct components: one CME related for lower energies and a second one for higher energies which is flare related (for the latter see the detail discussion in Kiselev et al. 2022).

Recent re-calibrations of science grade instruments further expanded the capabilities of space based detectors. For example, Kühl et al. (2017) demonstrated that the Electron Proton Helium Instrument (EPHIN) on board SOHO recorded 42 SEP events from 1997 to 2015 that reached a mean energy up to 610

KIEL-UP • DOI: 10.38072/2748-3150/p37

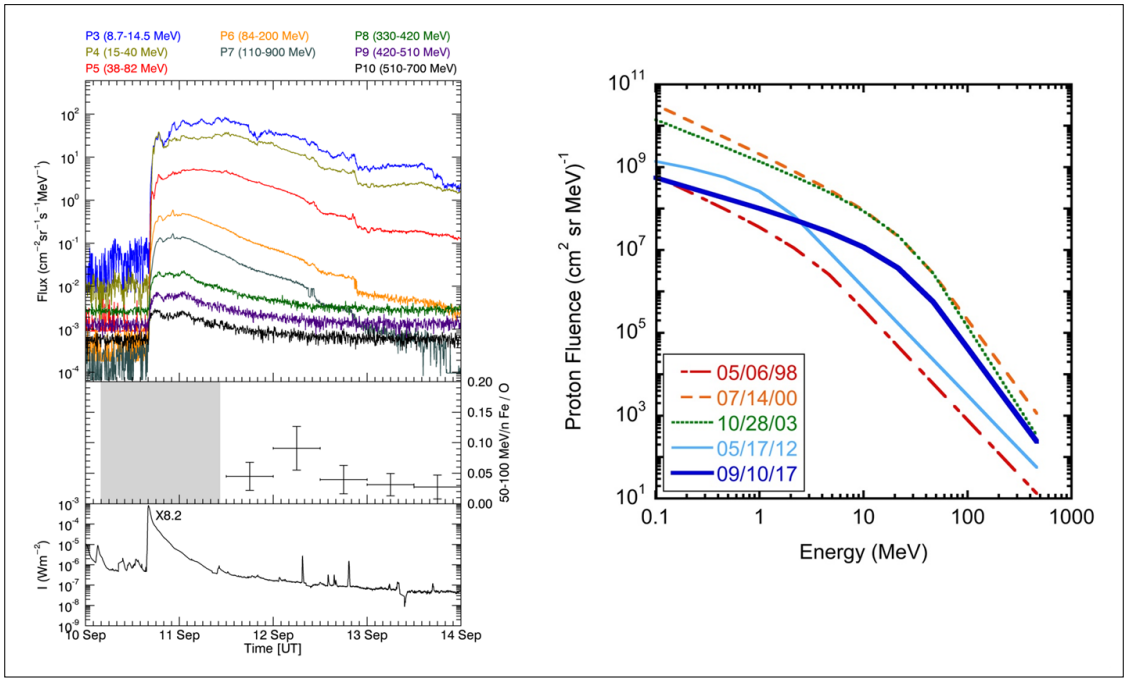

Fig. 11: Left panel: Recordings of the GLE72 on 10 September 2017 by (from top to bottom) GOES (8.7-700 MeV), SOHO/ERNE Fe/O at 50-100 MeV/n and GOES SXRs denoting the driving X8.2 solar flare (from Mishev et al. 2018). Right panel: Proton fluence spectrum for 5 GLEs obtained by GOES measurements demonstrating the double power law behavior (from Cohen and Mewaldt 2018).

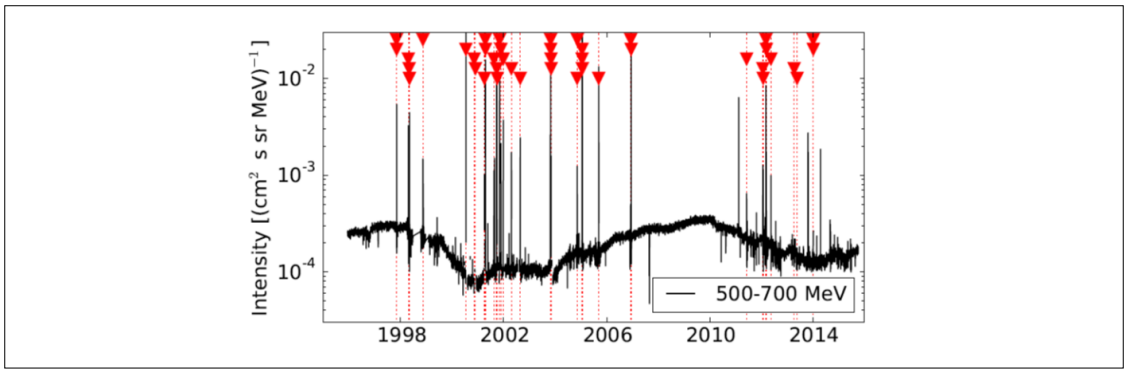

Fig. 12: Recordings of SOHO/EPHIN at 500-700 MeV from 1995-2015. The red triangles and the vertical lines denote the identified SEP events in these measurements (from Kühl et al. 2017).

MeV (Figure 12). A few of these SEP events were further recorded on the ground by NMs and thus were labeled as GLEs. Nonetheless, this paper gave rise to the identification of mildly relativistic particles and added context to the previously reported term: "sub-GLEs".[2] Moreover, most recently similar work has taken place for Solar Orbiter/HET and showed that particles up until ~890 MeV can be recorded, with most trusted ones reaching ~300 MeV. Both SOHO/EPHIN and Solo/HET measurements have been used in the identification of GLE73 (see Kouloumvakos et al. 2023). In addition, measurements from Payload for Antimatter Matter

2 See details in https://www.issibern.ch/teams/heroic/.

KIEL-UP • DOI: 10.38072/2748-3150/p37

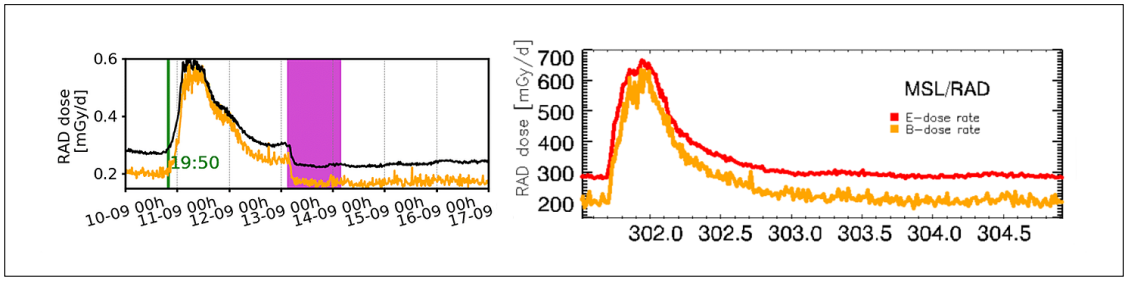

Fig. 13: Recordings of MSL/RAD at E>150 MeV demonstrating GLE72 (left panel; from Guo et al. 2018) and GLE73 (right panel; from Kouloumvakos et al. 2023).

Exploration and Light-nuclei Astrophysics (PAMELA) and the Alpha Magnetic Spectrometer (AMS)-02 payloads added significant information that bridges the critical gap in the spectra from the low-to-high energy particles (typically from about ~ 100 MeV to the NM range) (see e.g. Whitman et al. 2017; Bruno et al. 2018).

4.2 Recordings at different planets

100 years since the discovery of Cosmic Rays by Victor Hess in 1912, the Radiation Assessment Detector (RAD) onboard the Mars Science Laboratory (MSL) (Hassler et al. 2012) measures for the first time Cosmic Rays on the surface of another planet. This allowed us to observe solar particles reaching Mars at a few cases up to now with two of them being GLEs, i.e. GLE72 (Guo et al. 2018) and GLE73 (Kouloumvakos et al. 2023). As it can be seen in Figure 13 RAD onboard MSL on the surface of Mars recorded a distinguishable increase at both E- and B-dose rates (Hassler et al. 2012; Guo et al. 2015) for both GLEs. It should be noted that the required energy for the initiation of a proton triggering a GLE recorded by RAD located in Gale crater on Mars is ~ E>150 MeV (see Guo et al. 2018).

5. Future directions

5.1 GLEs as the stepping stone for super events

GLEs are hard spectrum events (Asvestari et al. 2017) and pose a significant threat for the radiation environment. Although, the Carrington event and its corresponding particle fluence were seen as the worst-case estimate of radiation hazard in the near-Earth environment that the Sun is capable of producing (Miroshnichenko & Nymmik 2014), with the help of cosmogenic radionuclide records, it became clear that much more extreme events (e.g. the event around AD774/775) might have occurred on the Sun (Miyake et al. 2012). Hence, these solar driven “super-events” are modeled on the basis of a multiplication factor of the measured GLE05 spectra. That said, GLEs provide direct context for the quantification and specification of the radiation environment during these “worst-case” scenario events.

5.2 GLEs contribution to the Sun-Earth-atmosphere system

The Sun-Earth connection is an intensive field of research for the past decades, GLEs provide a direct link to the atmospheric processes. For example, several works have focused on the ozone depletion (see the detailed work of Mironova et al. 2015) explaining the proposed mechanisms by which penetrating particles (i.e. not only of solar origin) can affect the atmosphere, including chemical changes in the upper atmo-

KIEL-UP • DOI: 10.38072/2748-3150/p37

sphere and lower thermosphere, chemistry-dynamics feedbacks, the global electric circuit (GEC) and cloud formation. Most recently, a study by Mallios et al. (2022) proposed a model of the atmospheric electricity and its variability during strong GLEs, demonstrating that in the case of fair weather conditions, GLE events enhance the atmospheric electrical conductivity, reduce the columnar resistance, and modify the fair weather electric field, air–earth conduction current, and possibly the Ionospheric Potential (IP) in a way that depends on the geomagnetic cut-off rigidity of the location and the altitude of the observer.

6. Conclusions

An overall presentation of Ground Level Enhancements (GLEs) has been provided in this work. Their historical identification and evolution of ideas for their origin; measurements from the worldwide neutron monitor network; modeling and forecasting efforts as well as their imprint in the inner heliosphere (on space based detectors and on the surface of Mars) together with a few future research directions have been presented. Thereby, if the question is, "What do we learn from GLEs?", the answer is that GLEs provide us with a direct link to access acceleration mechanisms at the Sun, to understand the solar storm evolution and to quantify their impact in the inner heliosphere and the near-Earth space, in particular. Additionally, GLEs pave the way for the understanding of the "worst-case" scenario for extreme SEP events and have further a direct impact on the atmospheric processes, which in turn, are directly related to the habitability of our planet and beyond.

Further contents

A Jupyter Notebook was implemented for this tutorial, accessible at: https://github.com/atpapaio/GLE-NMDB. It makes use of the script by C.T. Steigies (nest.py) to call NMDB and download data from the neutron monitor (NM) stations selected by the user (see also Steigies and Fuller 2023). The notebook (GLE_tutorail.ipynb) provides three plots:

- *First plot*: A percentage increase plot of the selected stations. In order to make the percentage a baseline (taken simply as the 1 hour, i.e. the first 60 minutes from the selected interval).
- *Second plot*: A plot of the North-South latitudinal anisotropy. Similar as before, in order to make the percentage a baseline (taken simply as the 1 hour, i.e. the first 60 minutes from the selected interval). Then, it makes a plot of two stations including their difference (the idea here is to directly evaluate the North-South latitudinal anisotropy. For this THULE and JBGO (or MCMU for earlier GLEs) should be selected, see also https://www.aanda.org/articles/aa/full_html/2022/04/aa42855-21/F10.html for an example).
- *Third plot*: This script provides the longitudinal anisotropy. Similar as before, in order to make the percentage a baseline (taken simply as the 1 hour, i.e. the first 60 minutes from the selected interval). The script makes a sum of all selected stations except the first one and then provides the difference between the first one and the rest of the NMs. The idea is to have all NM stations with a nominal cut-off Rc< 1.4 GV in order to evaluate the longitudinal anisotropy see also https://www.aanda.org/articles/aa/full_html/2022/04/aa42855-21/F11.html for an example).

KIEL-UP • DOI: 10.38072/2748-3150/p37

Acknowledgements

I would like to gratefully acknowledge the organizers for giving me the opportunity to give this tutorial on GLEs. The never-ending continuous efforts of the Neutron Monitor community at large and the Neutron Monitor Database (NMDB) in particular, without which our knowledge and understanding would be significantly hampered, are deeply appreciated. Constructive comments by Priv. Doc. Dr. Konstantin Herbst and the Organizing Committee of the NMDB@Athens 2022 (https://conf2022.nmdb.eu/) significantly improved the current manuscript. Discussions and exchange of ideas with Dr Christian T. Steigies and Mr George Vasalos helped shaping the accompanied python jupyter notebook on the analysis of GLEs for this tutorial. The present work benefited from discussions within the context of the ISSI International Team 441: High EneRgy sOlar partICle Events Analysis (HEROIC; https://www.issibern.ch/teams/heroic/).

References

Afanasiev, A., Vainio, R., Rouillard, A. P., Battarbee, M., Aran, A., & Zucca, P. (2018). Modelling of proton acceleration in application to a ground level enhancement. Astronomy & Astrophysics, 614, A4, https://doi.org/10.1051/0004-6361/201731343

Asvestari, E., Willamo, T., Gil, A., Usoskin, I. G., Kovaltsov, G. A., Mikhailov, V. V., & Mayorov, A. (2017). Analysis of Ground Level Enhancements (GLE): Extreme solar energetic particle events have hard spectra. Advances in Space Research, 60(4), 781-787, https://doi.org/10.1016/j.asr.2016.08.043

Belov, A., Eroshenko, E., Mavromichalaki, H., Plainaki, C., & Yanke, V. (2005). Solar cosmic rays during the extremely high ground level enhancement on 23 February 1956. In Annales Geophysicae (Vol. 23, No. 6, 2281-2291). Göttingen, Germany: Copernicus Publications, https://doi.org/10.5194/angeo-23-2281-2005

Benz A. O., Grigis P. C., Csillaghy A., Saint-Hilaire P. (2005). Survey on solar X-ray flares and associated coherent radio emissions. Solar Phys 226:121–142, https://doi.org/10.1007/s11207-005-5254-5

Bieber, J. W., Clem, J., Evenson, P., Pyle, R., Sáiz, A., & Ruffolo, D. (2013). Giant ground level enhancement of relativistic solar protons on 2005 January 20. I. Spaceship Earth observations. The Astrophysical Journal, 771(2), 92, https://doi.org/10.1088/0004-637X/771/2/92

Bombardieri, D. J., Duldig, M. L., Humble, J. E., & Michael, K. J. (2008). An improved model for relativistic solar proton acceleration applied to the 2005 January 20 and earlier events. The Astrophysical Journal, 682(2), 1315, https://doi.org/10.1086/589494

Bruno, A., Bazilevskaya, G. A., Boezio, M., Christian, E. R., de Nolfo, G. A., et al. (2018). Solar energetic particle events observed by the PAMELA mission. The Astrophysical Journal, 862(2), 97, https://doi.org/10.3847/1538-4357/aacc26

Bütikofer, R., Flückiger, E. O., Desorgher, L., & Moser, M. R. (2008). The extreme solar cosmic ray particle event on 20 January 2005 and its influence on the radiation dose rate at aircraft altitude. Science of the total environment, 391(2-3), 177-183, https://doi.org/10.1016/j.scitotenv.2007.10.021

Bütikofer, R., Agueda, N., Heber, B., Galsdorf, D., & Vainio, R. (2016). Assessment of Source and Transport Parameters of Relativistic SEPs Based on Neutron Monitor Data. arXiv preprint, https://doi.org/10.48550/arXiv.1612.08922

Bütikofer, R. (2018). Cosmic ray particle transport in the Earth's magnetosphere. Solar Particle Radiation Storms Forecasting and Analysis: The HESPERIA HORIZON 2020 Project and Beyond, 79-94, https://doi.org/10.1007/978-3-319-60051-2_5

Cane, H. V., Reames, D. V., & Von Rosenvinge, T. T. (1988). The role of interplanetary shocks in the longitude distribution of solar energetic particles. Journal of Geophysical Research: Space Physics, 93(A9), 9555-9567, https://doi.org/10.1029/JA093iA09p09555

Cane, H. V., & Lario, D. (2006). An introduction to CMEs and energetic particles. Space science reviews, 123(1-3), 45-56, https://doi.org/10.1007/978-0-387-45088-9_4

Cliver, E. W., & Herbst, K. (2018). Evolution of the sunspot number and solar wind B time series. Space Science Reviews, 214(2), 56, https://doi.org/10.1007/s11214-018-0487-4

Cohen, C. M. S., & Mewaldt, R. A. (2018). The ground level enhancement event of September 2017 and other large solar energetic particle events of Cycle 24. Space Weather, 16(10), 1616-1623, https://doi.org/10.1029/2018SW002006

Cramp, J. L., Duldig, M. L., Flückiger, E. O., Humble, J. E., Shea, M. A., & Smart, D. F. (1997). The October 22, 1989, solar cosmic ray enhancement: An analysis of the anisotropy and spectral characteristics. Journal of Geophysical Research: Space Physics, 102(A11), 24237-24248, https://doi.org/10.1029/97JA01947

Ellison, D. C., & Ramaty, R. (1985). Shock acceleration of electrons and ions in solar flares. The Astrophysical Journal, 298, 400-408, https://doi.org/10.1086/163623

Forbush, S. E. (1946). Three unusual cosmic-ray increases possibly due to charged particles from the Sun. Physical Review, 70(9-10), 771, https://doi.org/10.1103/PhysRev.70.771

Flückiger, E. O., & Kobel, E. (1990). Aspects of combining models of the Earth's internal and external magnetic field. Journal of geomagnetism and geoelectricity, 42(9), 1123-1136, https://doi.org/10.5636/jgg.42.1123

Flückiger, E. O., Moser, M. R., Pirard, B., Bütikofer, R., & Desorgher, L. (2008). A parameterized neutron monitor yield function for space weather applications. In International Cosmic Ray Conference (Vol. 1, 289-292), ID1182 (last accessed September 14, 2023)

Gopalswamy, N., Xie, H., Yashiro, S., Akiyama, S., Mäkelä, P., & Usoskin, I. G. (2012). Properties of ground level enhancement events and the associated solar eruptions during solar cycle 23. Space Science Reviews, 171, 23-60, https://doi.org/10.1007/s11214-012-9890-4

Guo, J., Zeitlin, C., Wimmer-Schweingruber, R. F., et al. (2015). Modeling the variations of dose rate measured by RAD during the first MSL Martian year: 2012–2014. The Astrophysical Journal, 810(1), 24, https://doi.org/10.1088/0004-637X/810/1/24

Guo, J., Dumbović, M., Wimmer Schweingruber, R. F., et al. (2018). Modeling the evolution and propagation of 10 September 2017 CMEs and SEPs arriving at Mars constrained by remote sensing and in situ measurement. Space Weather, 16(8), 1156-1169, https://doi.org/10.1029/2018SW001973

Hassler, D. M., Zeitlin, C., Wimmer-Schweingruber, R. F., et al. (2012). The radiation assessment detector (RAD) investigation. Space science reviews, 170, 503-558, https://doi.org/10.1007/s11214-012-9913-1

Herbst K. (2021). Exploring the Radiation and Particle Environment of Cool Stars and Their Impact on (Exo) Planetary Habitability, Habilitation Thesis, Christian-Albrechts-Universität zu Kiel.

Kiselev, V. I., Meshalkina, N. S., & Grechnev, V. V. (2022). Relationships Between the Spectra of Near-Earth Proton Enhancements, Hard X-Ray Bursts, and CME Speeds. Solar Physics, 297(5), 53, https://doi.org/10.1007/s11207-022-01986-7

Klein, K. L. (2021a). Radio astronomical tools for the study of solar energetic particles I. Correlations and diagnostics of impulsive acceleration and particle propagation. Frontiers in Astronomy and Space Sciences, 7, 580436, https://doi.org/10.3389/fspas.2020.580436

Klein, K. L. (2021b). Radio Astronomical Tools for the Study of Solar Energetic Particles II.Time-Extended Acceleration at Subrelativistic and Relativistic Energies Frontiers in Astronomy and Space Sciences, 7, 580436, https://doi.org/10.3389/fspas.2020.580445

Klein, K. L., Musset, S., Vilmer, N., et al. (2022). The relativistic solar particle event on 28 October 2021: Evidence of particle acceleration within and escape from the solar corona. Astronomy & Astrophysics, 663, A173, https://doi.org/10.1051/0004-6361/202243903

Kouloumvakos, A., Papaioannou, A., Vainio, R., Waterfall, C.O., Dalla, S., et al. (2023). The multi-spacecraft solar particle event on 28 October 2021. Astronomy & Astrophysics, under review.

Kühl, P., Dresing, N., Heber, B., & Klassen, A. (2017). Solar energetic particle events with protons above 500 MeV between 1995 and 2015 measured with SOHO/EPHIN. Solar Physics, 292, 1-13, https://doi.org/10.1007/s11207-016-1033-8

Kuwabara, T., Bieber, J. W., Clem, J., Evenson, P., & Pyle, R. (2006). Development of a ground level enhancement alarm system based upon neutron monitors. Space Weather, 4(10), https://doi.org/10.1029/2006SW000223

Mallios, S. A., Papaioannou, A., Herbst, K., Papangelis, G., & Hloupis, G. (2022). Study of the Ground Level Enhancements effect on atmospheric electric properties and mineral dust particle charging. Journal of Atmospheric and Solar-Terrestrial Physics, 233, 105871, https://doi.org/10.1016/j.jastp.2022.105871

Mavromichalaki, H., Papaioannou, A., Plainaki, C., et al. (2011). Applications and usage of the real-time Neutron Monitor Database. Advances in Space Research, 47(12), 2210-2222, https://doi.org/10.1016/j.asr.2010.02.019

McCracken, K. G., Moraal, H., & Shea, M. A. (2012). The high-energy impulsive ground-level enhancement. The Astrophysical Journal, 761(2), 101, https://doi.org/10.1088/0004-637X/761/2/101

Meyer, P., Parker, E. N., & Simpson, J. A. (1956). Solar cosmic rays of February, 1956 and their propagation through interplanetary space. Physical Review, 104(3), 768, https://doi.org/10.1103/PhysRev.104.768

Mewaldt, R. A., Looper, M. D., Cohen, C. M. S., et al. (2012). Energy spectra, composition, and other properties of ground-level events during solar cycle 23. Space Science Reviews, 171, 97-120, https://doi.org/10.1007/s11214-012-9884-2

Mironova, I. A., Aplin, K. L., Arnold, F., et al. (2015). Energetic particle influence on the Earth's atmosphere. Space science reviews, 194, 1-96, https://doi.org/10.1007/s11214-015-0185-4

Miroshnichenko, L. I. (2001). Solar cosmic rays (Vol. 2). Dordrecht/Boston: Kluwer Academic Publishers, https://doi.org/10.1007/978-94-015-9646-6

Miroshnichenko, L. I., & Nymmik, R. A. (2014). Extreme fluxes in solar energetic particle events: Methodological and physical limitations. Radiation Measurements, 61, 6-15, https://doi.org/10.1016/j.radmeas.2013.11.010

Mikić, Z., & Lee, M. A. (2006). An introduction to theory and models of CMEs, shocks, and solar energetic particles. Coronal Mass Ejections, 57-80, https://doi.org/10.1007/978-0-387-45088-9_5

Mishev, A. L., Usoskin, I. G., & Kovaltsov, G. A. (2013). Neutron monitor yield function: New improved computations. Journal of Geophysical Research: Space Physics, 118(6), 2783-2788, https://doi.org/10.1002/jgra.50325

Mishev, A., Usoskin, I., Raukunen, O., Paassilta, M., Valtonen, E., Kocharov, L., & Vainio, R. (2018). First analysis of ground-level enhancement (GLE) 72 on 10 September 2017: Spectral and anisotropy characteristics. Solar Physics, 293, 1-15, https://doi.org/10.1007/s11207-018-1354-x

Mishev, A., & Usoskin, I. (2020). Current status and possible extension of the global neutron monitor network. Journal of Space Weather and Space Climate, 10, 17, https://doi.org/10.1051/swsc/2020020

Mishev, A. L., & Velinov, P. I. Y. (2020). Ionization effect in the Earth's atmosphere during the sequence of October–November 2003 Halloween GLE events. Journal of Atmospheric and Solar-Terrestrial Physics, 211, 105484, https://doi.org/10.1016/j.jastp.2020.105484

Mishev, A. L., Koldobskiy, S. A., Kovaltsov, G. A., Gil, A., & Usoskin, I. G. (2020). Updated neutron monitor yield function: Bridging between in situ and ground based cosmic ray measurements. Journal of Geophysical Research: Space Physics, 125(2), e2019JA027433, https://doi.org/10.1029/2019JA027433

Mishev, A. L., Kocharov, L. G., Koldobskiy, S. A., Larsen, N., Riihonen, E., Vainio, R., & Usoskin, I. G. (2022). High-resolution spectral and anisotropy characteristics of solar protons during the GLE N◦ 73 on 28 October 2021 derived with neutron-monitor data analysis. Solar Physics, 297(7), 88, https://doi.org/10.1007/s11207-022-02026-0

Miyake, F., Nagaya, K., Masuda, K., & Nakamura, T. (2012). A signature of cosmic-ray increase in AD 774–775 from tree rings in Japan. Nature, 486(7402), 240-242, https://doi.org/10.1038/nature11123

Moraal, H., & McCracken, K. G. (2012). The time structure of ground level enhancements in solar cycle 23. Space Science Reviews, 171, 85-95, https://doi.org/10.1007/s11214-011-9742-7

Paassilta, M., Raukunen, O., Vainio, R., et al. (2017). Catalogue of 55–80 MeV solar proton events extending through solar cycles 23 and 24. Journal of Space Weather and Space Climate, 7, A14, https://doi.org/10.1051/swsc/2017013

Papaioannou, A., Souvatzoglou, G., Paschalis, P., Gerontidou, M., & Mavromichalaki, H. (2014). The first ground-level enhancement of solar cycle 24 on 17 May 2012 and its real-time detection. Solar Physics, 289, 423-436, https://doi.org/10.1007/s11207-013-0336-2

Papaioannou, A., Kouloumvakos, A., Mishev, A., et al. (2022). The first ground-level enhancement of solar cycle 25 on 28 October 2021. Astronomy & Astrophysics, 660, L5, https://doi.org/10.1051/0004-6361/202142855

Plainaki, C., Belov, A., Eroshenko, E., Mavromichalaki, H., & Yanke, V. (2007). Modeling ground level enhancements: Event of 20 January 2005. Journal of Geophysical Research: Space Physics, 112(A4), https://doi.org/10.1029/2006JA011926

Plainaki, C., Mavromichalaki, H., Belov, A., Eroshenko, E., Andriopoulou, M., & Yanke, V. (2010). A new version of the Neutron monitor based anisotropic GLE model: application to GLE60. Solar Physics, 264, 239-254, https://doi.org/10.1007/s11207-010-9576-6

Poluianov, S. V., Usoskin, I. G., Mishev, A. L., Shea, M. A., & Smart, D. F. (2017). GLE and sub-GLE redefinition in the light of high-altitude polar neutron monitors. Solar Physics, 292(11), 176, https://doi.org/10.1007/s11207-017-1202-4

Poluianov, S., & Batalla, O. (2022). Cosmic-ray atmospheric cutoff energies of polar neutron monitors. Advances in Space Research, 70(9), 2610-2617, https://doi.org/10.1016/j.asr.2022.03.037

Reames, D. V. (2009). Solar energetic-particle release times in historic ground-level events. The Astrophysical Journal, 706(1), 844, https://doi.org/10.1088/0004-637X/706/1/844

Rodriguez, J., & Kress, B. (2023). GOES Observations of Solar Protons during Ground Level Enhancements, this volume, https://doi.org/10.38072/2748-3150/p32

Shea, M. A., & Smart, D. F. (1982). Possible evidence for a rigidity-dependent release of relativistic protons from the solar corona. Space Science Reviews, 32, 251-271, https://doi.org/10.1007/BF00225188

Smart, D. F., Shea, M. A., & Flückiger, E. O. (2000). Magnetospheric models and trajectory computations. In Cosmic Rays and Earth: Proceedings of an ISSI Workshop, 21–26 March 1999, Bern, Switzerland (305-333). Springer Netherlands, https://doi.org/10.1023/A:1026556831199

Souvatzoglou, G., Papaioannou, A., Mavromichalaki, H., Dimitroulakos, J., & Sarlanis, C. (2014). Optimizing the real time ground level enhancement alert system based on neutron monitor measurements: Introducing GLE Alert Plus. Space Weather, 12(11), 633-649, https://doi.org/10.1002/2014SW001102

Steigies C.T. and Fuller N. (2023). Accessing NMDB data using NEST and pandas, this volume, https://doi.org/10.38072/2748-3150/p44

Temmer, M. (2021). Space weather: the solar perspective: An update to Schwenn (2006). Living Reviews in Solar Physics, 18(1), 4, https://doi.org/10.12942/lrsp-2006-2

Tsyganenko, N. A. (1989). A magnetospheric magnetic field model with a warped tail current sheet. Planetary and Space Science, 37(1), 5-20, https://doi.org/10.1016/0032-0633(89)90066-4

Usoskin, I., Koldobskiy, S., Kovaltsov, G. A., Gil, A., Usoskina, I., Willamo, T., & Ibragimov, A. (2020). Revised GLE database: Fluences of solar energetic particles as measured by the neutron-monitor network since 1956. Astronomy & Astrophysics, 640, A17, https://doi.org/10.1051/0004-6361/202038272

Vainio, R., & Laitinen, T. (2007). Monte Carlo simulations of coronal diffusive shock acceleration in self-generated turbulence. The Astrophysical Journal, 658(1), 622, https://doi.org/10.1086/510284

Vainio, R., Valtonen, E., Heber, B., et al. (2013). The first SEPServer event catalogue~ 68-MeV solar proton events observed at 1 AU in 1996–2010. Journal of space weather and space climate, 3, A12, https://doi.org/10.1051/swsc/2013030

Vashenyuk, E. V., Balabin, Y. V., & Gvozdevsky, B. B. (2011). Features of relativistic solar proton spectra derived from ground level enhancement events (GLE) modeling. sAstrophysics and Space Sciences Transactions, 7(4), 459-463, https://doi.org/10.5194/astra-7-459-2011

Vlahos, L., Anastasiadis, A., Papaioannou, A., Kouloumvakos, A., & Isliker, H. (2019). Sources of solar energetic particles. Philosophical Transactions of the Royal Society A, 377(2148), 20180095, https://doi.org/10.1098/rsta.2018.0095

Vourlidas, A. (2021). Improving the Medium-Term Forecasting of Space Weather: A Big Picture Review From a Solar Observer's Perspective. Frontiers in Astronomy and Space Sciences, 8, 651527, https://doi.org/10.3389/fspas.2021.651527

Whitman, K., Bindi, V., Consolandi, C., Corti, C., & Yamashiro, B. (2017). Implications of improved measurements of the highest energy SEPs by AMS and PAMELA. Advances in Space Research, 60(4), 768-780, https://doi.org/10.1016/j.asr.2017.02.042

Wild, J. P., Smerd, S. F., & Weiss, A. A. (1963). Solar bursts. Annual Review of Astronomy and Astrophysics, 1(1), 291-366, https://doi.org/10.1146/annurev.aa.01.090163.001451

Yashiro, S., Akiyama, S., Gopalswamy, N., & Howard, R. A. (2006). Different power-law indices in the frequency distributions of flares with and without coronal mass ejections. The Astrophysical Journal, 650(2), L143, https://doi.org/10.1086/508876

Open Access